ORIGINAL ARTICLE

Influence of In Vitro Electrical Stimulation on Survival of Spiral Ganglion Neurons

Marvin N. Peter [1] · Athanasia Warnecke [1,2] · Uta Reich [3] · Heidi Olze [3] · Agnieszka J. Szczepek [3] · Thomas Lenarz [1,2] · Gerrit Paasche [1,2]

Abstract

Patients scheduled for cochlear implantation often retain residual hearing in the low frequencies. Unfortunately, some patients lose their residual hearing following implantation and the reasons for this are not well understood. Evidence suggests that electrotoxicity could be one of the factors responsible for this late adverse effect. Therefore, the aim of this study was to investigate the survival of spiral ganglion neurons (SGN) subjected to in vitro electrical stimulation (ES). A stimulation setup was developed to provide defined electrical fields at given points of the chamber. SGN isolated from Sprague Dawley rats (P3–4) were dissociated and cultured in the chamber for 24 h prior to biphasic, pulsed electrical field exposure for another 24 h. The current varied in the range of 0 to 2 mA and the pulse width from 10 to 400 µs. Neurite growth and survival were evaluated with respect to the charge density at the position of the cells. Non-exposed SGN cultures served as control. Charge densities below 2.2 $\mu C \cdot cm^{-2} \cdot phase^{-1}$ appeared to have no effect on SGN survival and neurite outgrowth. Charge densities above 4.9 $\mu C \cdot cm^{-2} \cdot phase^{-1}$ were detrimental to almost all cells in culture. After fitting results to a sigmoidal dose response curve, a LD_{50} of 2.9 $\mu C \cdot cm^{-2} \cdot phase^{-1}$ was calculated. This screening regarding survival and outgrowth of SGN provides parameters that could be used to further investigate the effect of ES on SGN and to develop possible protection strategies, which could potentially rescue residual hearing in the implanted patients.

Introduction

Sensorineural hearing loss is characterised by the loss of inner and outer hair cells. This is often accompanied by the degeneration of spiral ganglion neurons (SGN). A first choice treatment for moderate hearing loss would be amplification of stimulus via a hearing aid. However, in some cases, the hearing loss is more severe and a cochlear implant (CI) is the only option to elicit a hearing sensation in the patient. When using a CI, an electrode array is inserted into the *scala tympani* for direct electrical stimulation of residual SGN. Only conditions with hair cell loss but preservation of at least some of the SGN can therefore be treated with a CI. Due to the overall good results with a CI, more and more patients with residual hearing lacking sufficient speech perception also receive cochlear implants. Residual hearing can be preserved in 59% of patients (Jurawitz et al. 2014). Nevertheless, a significant proportion of patients lose their residual hearing following implantation (Kopelovich et al. 2015). Early loss of residual hearing might be the result of damage and inflammation due to insertion trauma and foreign body reaction. However, some of the patients lose their residual hearing in the long term after initial preservation (Santa Maria et al. 2013; Skarzynski et al. 2013; Helbig et al. 2016). Although this phenomenon is clinically relevant, there is a lack in research addressing its aetiology.

✉ Athanasia Warnecke
Warnecke.Athanasia@mh-hannover.de

1   Department of Otorhinolaryngology, Head and Neck Surgery, Hannover Medical School, Stadtfelddamm 34, 30625 Hannover, Germany

2   Cluster of Excellence "Hearing4all" of the German Research Foundation, Oldenburg, Germany

3   Department of Otorhinolaryngology, Head and Neck Surgery, Berlin Institute of Health, Charité - Universitätsmedizin Berlin, Corporate Member of Freie Universität Berlin, Humboldt-Universität zu Berlin, Berlin, Germany

Several experimental studies have shown that electrical stimulation (ES), especially when combined with growth factors, has a protective effect on SGN (Lousteau 1987; Hartshorn et al. 1991; Leake et al. 1991; Mitchell et al. 1997). For electrical stimulation alone, an improved survival of SGN was shown (Scheper et al. 2009). But the clinical observations with late loss of residual hearing have challenged the idea of ES being protective.

One of the possible reasons explaining the aetiology of late post-implantation residual hearing loss could be the excitotoxicity or electrotoxicity to hair cells or SGN at certain combinations of stimulation parameters. In some studies, degeneration of nerve fibres and synapses after noise trauma was shown to be the result of excessive glutamate release (Puel et al. 1998; Kujawa 2006; Kujawa and Liberman 2009; Stalmann 2015). Other neuronal systems such as retinal ganglion cells in the eye may also be affected by excitotoxicity. A local high exposure to glutamate causes degeneration of the corresponding nerve cells (Olney et al. 1971; Sucher et al. 1997; Liberatore et al. 2017). Moreover, well known are the glutamate-induced changes in the hippocampus, for which various ways of prevention are investigated (Rosso et al. 2017; Budni et al. 2018). In addition to excitotoxicity, the cells could be damaged directly by electric current. Our own preliminary work in an in vitro system provides initial indications of electrotoxicity caused by ES (Reich et al. 2015) that could be involved in the late loss of residual hearing. In the study mentioned, preparations of the organs of Corti containing hair cells, the SGN showed degeneration after 42 h of electrical stimulation. The positive effects of electrical stimulation have also been observed. Thus, a positive impact was found by electrical neuromuscular stimulation on pulmonary function in patients on haemodialysis (Roxo et al. 2016). Two other examples of the supporting ability of electrical stimulation are mentioned below. Targeted electrical stimulation can more quickly reduce the incidence of post-stroke dysphagia and support logopaedic therapy (Dziewas et al. 2018). Furthermore, electrical stimulation can also help wound healing of the skin (Long et al. 2018). The precise stimulation parameters that would induce excitotoxicity or electrotoxicity have not been sufficiently studied yet. A safe stimulation area was determined based on safe and unsafe electrical stimulation levels for surface electrodes on the cortex in vivo (Shannon 1992). However, such investigations for the cochlear neurons are not available hitherto.

This study was designed to establish an in vitro assay utilising a chamber with a radial electric field for in vitro electrical stimulation of SGN from postnatal rats as a screening tool. In this experimental setting, parameters such as current amplitude and pulse width could be varied in order to delineate potentially protective or toxic parameters of ES on SGN. For ethical reasons, we refrained from using an in vivo model for screening experiments.

Materials and Methods

Ethical Approval

All applicable international, national, and/or institutional guidelines for the care and use of animals were followed. This article does not contain any studies with human participants performed by any of the authors. All experiments were carried out according to the German "Law on Protecting Animals" (§4) and with the European Directive 2010/63/EU for protection of animals used for experimental purposes. These experiments are registered (No. 2016/118) with the local authorities (Laboratory Animal Science).

Preparation and Dissociation of Spiral Ganglion Neurons

Postnatal (P3–4) Sprague Dawley rats of different sexes were used for in vitro culture. The rats were decapitated, the skull opened, the brain removed and the petrous bone placed in a Petri dish (60 × 15 mm, GREINER BIO-ONE, Nenndorf, Germany) with ice-cold Ca^{2+}/Mg^{2+}-free D-phosphate buffer (PBS, Gibco® THERMO FISHER SCIENTIFIC, Waltham, Massachusetts, USA). The membranous cochlea was uncovered from the petrous bone, and subsequently the spiral ganglion (ganglion spirale cochleae) was transferred in an ice-cold Ca^{2+}/Mg^{2+}-free Hank's solution (HBSS, INVITROGEN, Carlsbad, California, USA) (Warnecke et al. 2012).

The collected spiral ganglia of $15-20$ rats were enzymatically and mechanically dissociated. The pooled spiral ganglia were transferred to a HBSS solution containing 0.1% trypsin (BIOCHROM, Berlin, Germany) and 0.01% DNase I (ROCHE, Basel, Switzerland) and incubated for 16 min at 37 °C and 5% CO_2. The dissociation was stopped with pre-warmed fetal calf serum (FCS Superior, BIOCHROM), and the agglomerates were washed with serum-free medium to remove FCS, trypsin and DNase I. The following substances were used to prepare the serum-free medium: Panserin 401 (PAN BIOTECH, Aidenbach, Germany), HEPES Puffer (23.4 μmol/mL, INVITROGEN), PBS (0.172 mg/mL), penicillin (30 U/mL, BIOCHROM), glucose (0.15%, B. BRAUN, Melsungen, Germany), insulin (8.7 μg/mL, BIOCHROM) and N-2 supplement (0.1% INVITROGEN). The cells were triturated mechanically in 1 mL of serum-free medium by drawing them in and out of 1000 μL, and then a 200 μL pipette (pipette tips TipOne®, STARLAB, Hamburg, Germany) until a homogeneous solution was obtained. Finally, the number of viable cells was determined using the Trypan Blue Exclusion Assay (SIGMA-ALDRICH, St. Louis, Missouri, USA) in a NEUBAUER chamber (BRAND GmbH, Wertheim, Germany). In the end, the cell suspension (spiral ganglion cell mixed culture, SGC culture) was centred on a coated Petri dish (diameter: 35 mm, TPP, Trasadingen, Switzerland) at a concentration of $3.5 \cdot 10^4$ cells/mL. The

coating consisted of 0.1 mg/mL poly-DL-ornithine hydrobromide (Sigma-Aldrich) and 0.01 mg/mL mouse laminin, natural (Invitrogen) (Schwieger et al. 2016). The cell suspension rested for 1 h in the incubator, and dishes were then filled with 10% FCS up to a volume of 2 mL with serum-free medium.

Culture and Stimulation of Spiral Ganglion Neurons

For electrical stimulation, specially developed stimulation chambers were used. The chambers have a central electrode (diameter $0.50 \pm 9.3 \cdot 10^{-3}$ mm) and a ring electrode (radius 10.83 ± 0.27 mm) both consisting of 900/100 platinum-iridium wire. This material is biocompatible and inert to biological tissue (Habel 2004). Both electrodes are fixed in a glass lid (Fig. 1a), which replaces the lid of a regular Petri dish. By positioning the glass lid on the Petri dish, the electrodes are touching the bottom of the Petri dish. Thus, the cells are seeded and grow on the bottom of the dish directly between both electrodes. The central electrode was partly covered with a silicone tube for insulation, so that only a 1 mm long tip remained free. A grid (Fig. 1b) was attached to the outside of the bottom of the Petri dishes to ease later evaluation. A hydrophobic barrier (ImmEdge Hydrophobic Barrier PAP Pen, Vector Laboratories, Burlingame, California, USA) was applied with a radius of 1 cm around the central electrode to limit cell distribution in the dish. To indicate the distribution of the electric charge density within the dish, a finite element analysis (software QuickField, Tera Analysis Ltd., Svendborg, Denmark) was performed (Fig. 1c). The charge density is used as a parameter that could indicate the stress level the cells are exposing. In order to reuse the developed electrodes, they were cleaned and sterilised after each experiment.

A pulse generator (10 -MHz Pulse Generator TGP 110, Aim-TTi, Cambridgeshire, United Kingdom) was used for electrical stimulation to generate the electrical, rectangular pulse. An oscilloscope (HM 307-4, Hameg, Mainhausen, Germany) was used to monitor the current waveform and an amplitude modulator (constructed in house by the Central Research Devices Service Unit) was used to provide a constant amplitude. The amplitude modulator also changed the polarity of every second pulse for biphasic stimulation. The modules and the samples were connected together as schematically demonstrated in Fig. 2.

In each experimental series, two cultures were exposed to ES and another two were used as controls. The cells were placed in an incubator (Thermo Fisher Scientific) at 37 °C and 5% CO_2 in a serum-free medium (see above). After 24 h, stimulation electrodes were inserted in the middle of the wells and connected with the stimulation setup. No electrodes were inserted into the controls. For stimulation, the amplitude was varied between 0 and 2 mA and the pulse widths between 10 and 400 μs. The inter-pulse delay was 120 μs and the repetition rate was 1 kHz. The stimulation was stopped after further 24 h and the cells were fixed with a 1:1 (v:v) mixture of methanol (≥ 99.9%, Carl Roth, Karlsruhe, Deutschland) and acetone (≥ 99.9%, Sigma-Aldrich). Three repetitions per stimulation parameter were performed with two stimulated dishes each.

For a compatibility test, an independent series of experiments was carried out. In order to exclude that the material, of which the stimulation electrode was made of, has an influence on SGN survival or neurite outgrowth, the stimulation electrodes were inserted into the Petri dishes but were not switched on. To control for this possible effect, three separate experiments were performed.

In order to exclude heating due to electrical stimulation, the temperature was measured during electrical stimulation with a temperature sensor (HH-25TC, Omega, Stamford, Connecticut, USA) positioned at a distance of 1 mm from the centre electrode and fastened to the cover of the electrode. In this experiment, no cells but only serum-free medium was used. The Petri dish with medium was placed in the incubator
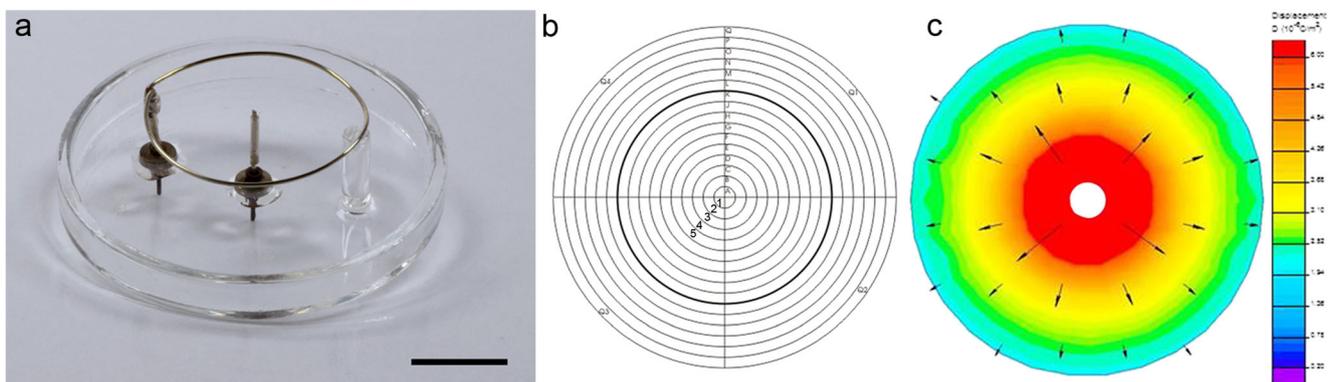

Fig. 1 a Stimulation chamber with a central electrode and a ring electrode in a glass lid (scale bar 10 mm), b Evaluation grid with radii at a distance of 1 mm (effective range 1 – 5 mm). Thick line marks a radius of 10 mm, c Finite element analysis (software QuickField) of the electric charge density distribution during stimulation. The colour coding shows the strength of the electric charge density decreasing from centre to ring electrodes. The arrows indicate the radial electric field
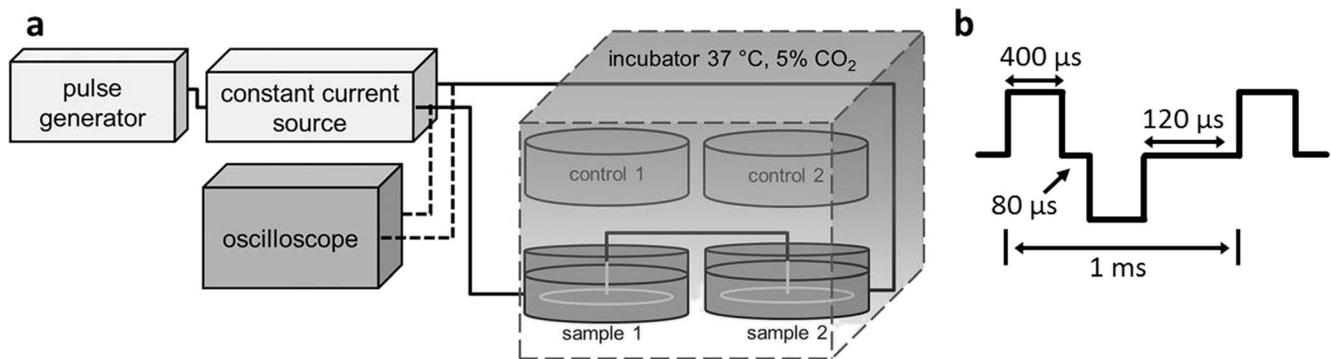
Fig. 2 Stimulation setup. **a** For the experiments, two samples were connected in row and electrically stimulated and two controls were not stimulated. **b** Example of pulse parameters for the electrical stimulation

for 24 h before stimulation with current of 2 mA and 400 µs pulse width.

Immunocytochemistry and Image Analysis

The SGC culture is a mixed culture and consists of the spiral ganglion neurons and a variety of other cell types, e. g., fibroblasts and glial cells. For this reason, a specific staining is necessary. For the study of neuronal survival and neurite length in the SGC culture, the neurofilament of the SGN was specifically labelled with a mouse 200 kDa neurofilament primary antibody (Novocastra®, Leica, Wetzlar, Germany) and with a secondary biotinylated anti-mouse antibody (Vectastain®, Vector Laboratories). Subsequently the Vectastain® Elite® ABC kit (Vector Laboratories) and 3,3′-diaminobenzidine (DAB) (Peroxidase Substrate Kit DAB, Vector Laboratories) were used for visualisation (Warnecke et al. 2012). For image acquisition, an inverse microscope (BZ-9000, Keyence, Neu-Isenburg, Germany) and the accompanying software BZ-II Viewer and BZ-II Analyser were used. The software ImageJ (National Institutes of Health, Bethesda, USA) was used to measure the length of the neurites. Spiral ganglion neurons that have a neurite three times longer than the diameter of the soma were defined as surviving (Gillespie et al. 2001). SGN were counted and measured within a radius of 1 – 5 mm from the central electrode. If the soma of a cell grew on the radius-marking line of the evaluation grid, it was counted to the next lower radius. Both cell survival and neurite length of the SGN were examined with respect to current amplitude and pulse width. To investigate the effect of changes in pulse width, a current of 1 mA was kept constant. When testing the current amplitude, a pulse width of 400 µs was used. For neuronal morphology, the SGN were examined for their polarity. According to the study by Whitlon et al. 2007, four groups were defined: monopolar, bipolar, pseudomonopolar and multipolar. Appearances of the four different morphologies were calculated as percentage of the total number of countable SGN (Schwieger et al. 2015).

The charge density σ (1) for the applied current amplitude I and pulse width t were calculated for each position $r_{1-5\ mm}$ between the central electrode and the ring electrode based on the radial electric field. The height h of the respective cylinder was approximated by the length of the non-isolated central electrode (1 mm).

$$\sigma = \frac{I \cdot t}{2\pi r h} \tag{1}$$

To determine the relative SGN survival rate (2) and the relative neurite length (3), the mean values were calculated from the length and survival of unstimulated and stimulated SGN cultures from the same experiment.

$$\text{rel.survival rate} = \frac{\text{survival}_{\text{stimulated}}}{\text{survival}_{\text{unstimulated}}} \tag{2}$$

$$\text{rel.neurite length} = \frac{\text{neurite length}_{\text{stimulated}}}{\text{neurite length}_{\text{unstimulated}}} \tag{3}$$

The three-dimensional diagrams were created using the OriginPro 9.1 (OriginLab, Massachusetts, USA) spreadsheet software.

Statistical Evaluation

For statistical analyses, data were tested for linear correlation according to Pearson and normal distribution according to Kolmogrov-Smirnov. Data were analysed using one-way ANOVA and subsequent Tukey multiple comparison. In addition, the paired t test was used to compare the unstimulated and stimulated SGN cultures. The lethal dose (LD_{50}) was determined by fitting the data to a sigmoidal survival curve. Spreadsheet software was Prism 5 (GraphPad®, La Jolla, California, USA). The data are presented as mean $\bar{x} \pm$ standard error of the mean (SEM). Each variation of the pulse was repeated in triplicate ($N = 3$). The number of cells n varied according to the applied parameters and is identified in the results. Differences were considered to be significant when the probability of error α was below 5% ($p < 0.05$).

Results

Compatibility of Experimental Setup

To test the experimental setup for cytocompatibility, SGN were cultured in a Petri dish containing culture medium supplemented with FCS and the other factors as described above in the absence (without electrode) and presence (with electrode) of the stimulating electrode but without current. The number of cells increased with the radius as expected due to the larger culture surface. There was no difference between the two conditions (with and without electrode; Fig. 3a). Cells cultured in the absence of an electrode array had an average neurite length of 236.5 ± 2.56 μm across all radii compared to 223.0 ± 7.46 μm with electrode. There was no significant difference in neurite length between the two conditions (with and without electrode) except for radius 4 mm and 5 mm (Fig. 3b). With radius 4 mm, the neurite length was 235.0 ± 5.60 μm without electrode and decreased slightly but significantly to 207.6 ± 5.06 μm in the presence of the electrode array (Fig. 3b) and for radius 5 mm from 230.8 ± 4.86 μm to 207.9 ± 4.72 μm respectively. Nevertheless, all radii were used for the investigation, and the samples with electrode were used as reference value by using Eqs. (2) and (3).

When testing for heating during electrical stimulation, only temperature fluctuations of ± 0.1 °C were found and no longer taken into account as a potentially damaging factor (data not shown).

Influence of Current Amplitude on SGN

The same setting as above was used with the electrode array activated for stimulating SGN. Unstimulated SGN were cultured in a Petri dish in the absence of an electrode array (unstimulated). Transmitted light microscopic images of the stained SGN illustrate differences in survival and morphology following electrical stimulation (Fig. 4). The unstimulated SGN culture is shown in Fig. 4a. Electrical stimulation using a current of 0.33 mA had no visible effect on the SGN cells

regarding their number and neurite length, as compared to the unstimulated culture (Fig. 4b). Electrical stimulation using a current of 1.0 mA clearly decreased the survival and the length of neurites of SGN cells (Fig. 4c). After electrical stimulation using a current of 2.0 mA, no surviving SGN could be detected in the inner radius (Fig. 4d).

Figure 5 depicts the relative neuronal survival under electrical stimulation for 24 h with different current amplitudes ranging from 0.084 to 2.0 mA and a charge density from 0.2 to 18 μC·cm^{-2}·phase^{-1}. The survival was set in relation to the neuronal survival of unstimulated cells (reference). In the amplitude range of $0.084 - 0.17$ mA, the rel. survival rates were similar to those in the references. By contrast, the currents 0.25 mA at a charge density of $0.6 - 1.0$ μC·cm^{-2}·phase^{-1} indicated a trend towards protective effects on spiral ganglion neurons. For example, rel. survival rates of up to 205% relative to the corresponding controls at 0.61 μC·cm^{-2}·phase^{-1} and 0.25 mA were quantified, even though this was not significant. On the other hand, there was already a strong trend towards lower rel. survival rates between 0.33 and 0.44 mA at a higher charge density of $2.4 - 3.0$ μC·cm^{-2}·phase^{-1}. Increasing the charge density over 4.7 μC·cm^{-2}·phase^{-1} resulted in a significant decrease in rel. Neuronal survival rates ($p < 0.05$; Table 1). The only exception was 1 mA at 1 mm from the centre (rel. survival as low as 9.5%). At a current amplitude of 2.0 mA, only a few neurons survived (max. 5.4%). Applying 0.88 mA resulted in a much better cell survival compared to all other currents at similar charge densities. When calculating LD$_{50}$ values, these had to be left out in order to be able to fit a survival curve. The LD$_{50}$ was then calculated to be at a charge density of 2.9 μC·cm^{-2}·phase^{-1}. For a better overview, all significant differences are listed in Table 1.

The neurite length of surviving SGN was measured in the stimulated as well as in unstimulated samples. The relative neurite length was calculated ($\frac{stimulated}{unstimulated}$). In Fig. 6a, the parameters (relative neurite length, radius and current amplitude) combine to form a map. The influence of the current and the distance to the central electrode on the neurite length becomes particularly clear on the map. If

Fig. 3 Compatibility experiment for testing potential toxicity of the electrode material on SGN. **a** Survival of SGN in relation to the distance from the centre of the Petri dish. The number of cells increased with radius due to the larger area (inset Fig. 3a). **b** Neurite length as function of the distance from the centre electrode. Differences become significant for radii 4 mm and 5 mm. * $p < 0.05$
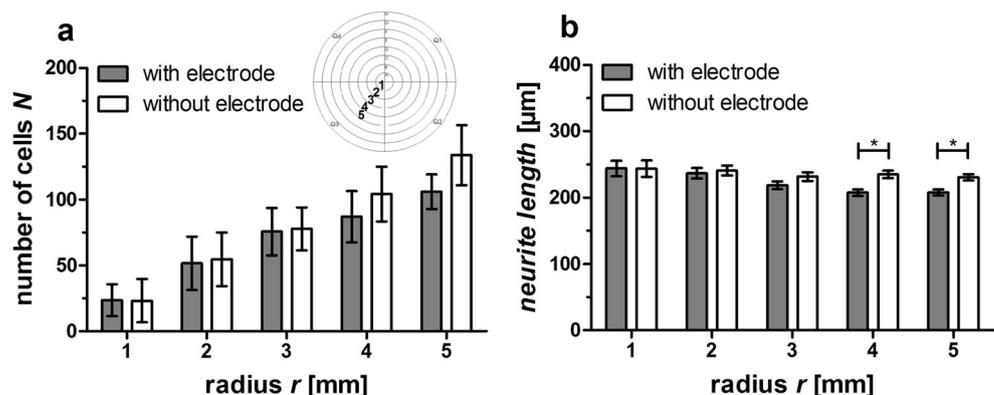
Fig. 4 Transmitted light microscopic images of SGN after 2 days in culture. **a** Unstimulated SGN culture without stimulation chamber. **b** SGN culture stimulated with 0.33 mA. The morphology of SGN is similar to the unstimulated SGN culture. **c** SGN culture stimulated with 1.0 mA (visible decline of SGN survival and neurite length) **d** SGN culture stimulated with 2.0 mA. No survival of SGN at short distances from the centre electrode. In Figure **b**, **c** and **d**, the outlines of the grid located below the bottom of the Petri dish are visiable as dark semicircles. Scale bar 200 μm. The arrow indicated the direction of the centre electrode
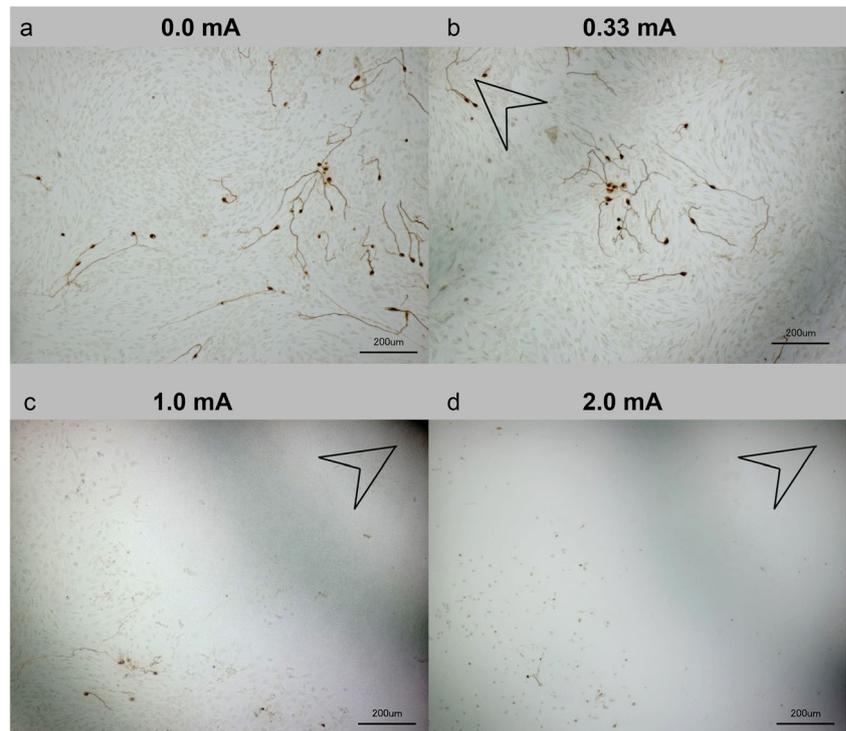
the distance to the central electrode was short and the current amplitude high, the relative neurite length was shorter. At an amplitude of 0.44 mA and 0.88 mA, a trend towards shorter neurites compared to the unstimulated culture was already observed. At a current level of 1 mA and a charge density of $3.8 - 5.4$ μC·cm^{-2}·phase^{-1} (2 – 3 mm radius), the difference to the corresponding unstimulated SGN culture is significant ($p < 0.05$). There is a linear correlation between the charge density and the neurite length (Fig. 6b). At a charge density of 8.9 μC·cm^{-2}·phase^{-1} (1 mm radius), the neurite outgrowth of SGN was reduced and the longest measured neurites were as short as 36.7 μm (unstimulated $= 171.5 \pm 17.4$ μm) (Fig. 6b). The SGN reacted even more strongly at 2 mA to the resulting charge

Fig. 5 **a** Relative SGN survival with different stimulation current amplitudes over 24 h. The measuring points of the individual currents can be read from right to left as follows: [1, 2, 3, 4, 5] mm. $n = 0 - 95$. The fitted curve comprises all data shown with the exception of the 0.88 mA measurement. For the fit, the upper limit was set to 100% and 0% as lower limit. Detailed diagrams with error bars are shown in **b**, **c** and **d**, means ± standard error of the mean (SEM). Significant differences are specified in Table 1
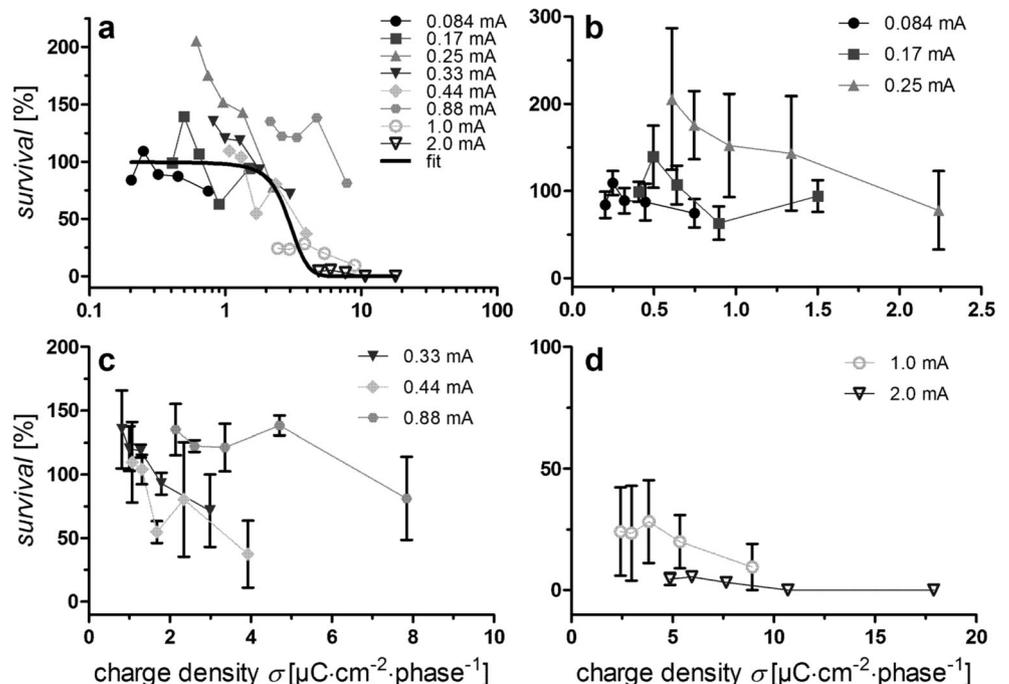
Table 1 Statistical analyses of rel. SGN survival. On the left side one-way ANOVA (post-test: TUKEY multiple comparison) was used to compare rel. cell survival for all applied currents for the different distances (radius) from the centre electrode. The right hand side of the table provides significant differences between stimulated and the respective unstimulated samples. All other differences were not significant. $*p < 0.05$; $**p < 0.01$; $***p < 0.001$

One-way ANOVA			t test		
Radius [mm]	Pairing (stimulated)	Significance	Radius [mm]	Pairing (unstimulated/stimulated)	Significance
2	0.88 mA + 2.0 mA	*	2	0.17 mA	*
3	0.25 mA + 2.0 mA	*	2	1.0 mA	*
3	0.88 mA + 2.0 mA	*	2	2.0 mA	*
4	0.25 mA + 1.0 mA	*	3	2.0 mA	***
4	0.25 mA + 2.0 mA	*	4	2.0 mA	**
4	0.88 mA + 2.0 mA	*	5	2.0 mA	*
5	0.25 mA + 2.0 mA	*			

density. The neurite length of SGN was even shorter (max. 102.0 ± 15 µm at a charge density of 5.9 µC·cm^{-2}·phase^{-1}; 4 mm radius). From a charge density of 8.0 µC·cm^{-2}·phase^{-1} and above, no SGN survived electrical stimulation. For the larger radii ($4 - 5$ mm), the reduction in neurite length was significant (Fig. 6c).

Fig. 6 Relative neurite length after electrical stimulation at different current levels over 24 h. **a** Parameter space over different currents and radii. **b**, **c**. Detailed representations of results at 1 mA (**b**) and 2 mA (**c**) with corresponding charge density at the respective stimulation site, means ± standard error of the mean (SEM) (**b**, **c**) and 95% confidence interval (**b**), $n = 0 - 95$. $*p < 0.05$, $***p < 0.001$
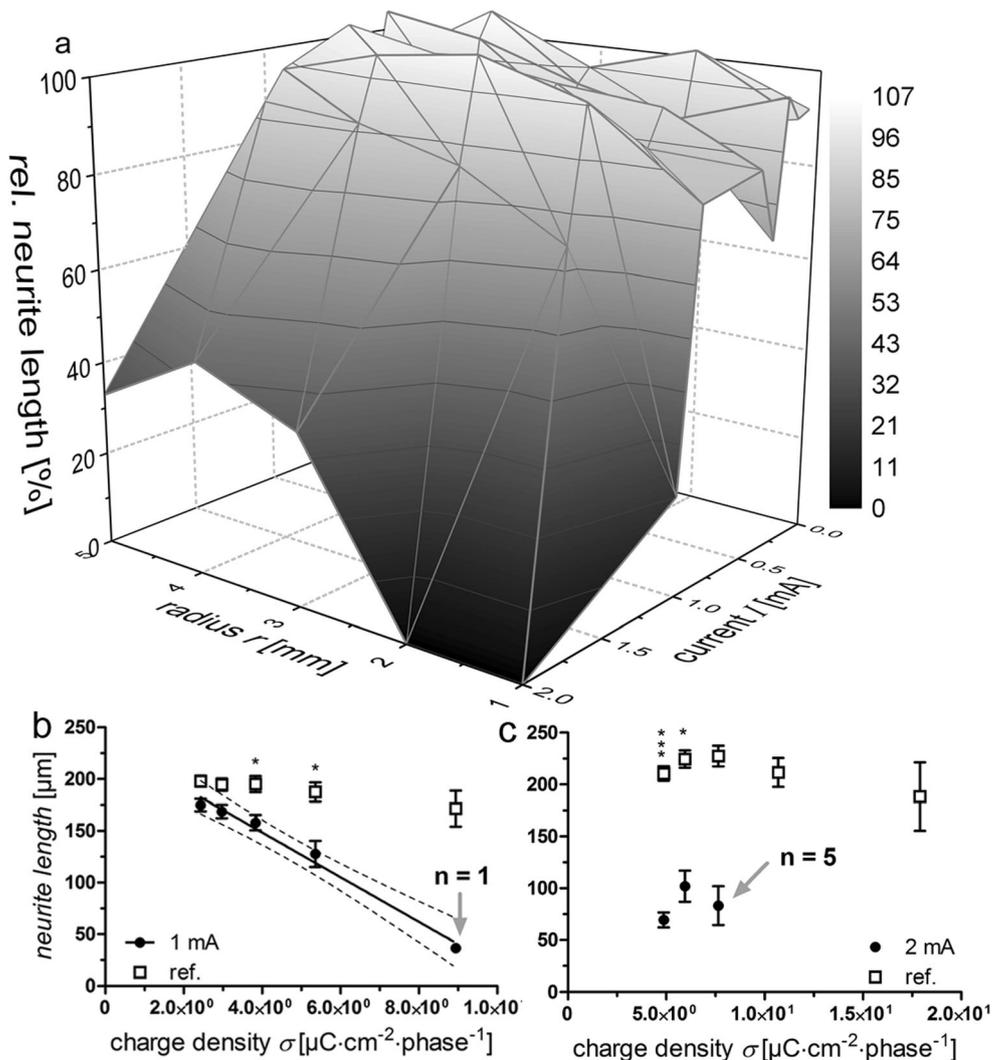
Influence of Pulse Width on SGN

Relative survival of SGN and outgrowth of neurites was investigated under electrical stimulation and variation of pulse width. The current amplitude was constant at 1 mA. The rel. survival rates of the SGN at a pulse width of 10 μs and 100 μs were compared to the rel. survival rates obtained without stimulation. Relative survival rates of the SGN at pulse widths of 10 μs and 100 μs increased to 182% at a charge density of 1.3 μC·cm^{-2}·phase^{-1} compared to the unstimulated references. Further increase of pulse width by fourfold (to 400 μs) and a resulting charge density of 2.4 to 8.9 μC·cm^{-2}·phase^{-1} induced a strong decrease of the rel. SGN survival rate to 9.5% (Fig. 7).

Pulse width had similar influence on neurite length as on the cell survival (Fig. 8). The three-dimensional diagram shows the complete tested parameter range (Fig. 8a). At a pulse width of 10 and 100 μs, the average relative neurite length was 97%. Increasing the pulse width and approaching the central electrode decreases the relative neurite length. In addition, the pulse width variation has a similar influence on the neurite length, as does the current amplitude (c.f. Fig. 6a). If the distance to the centre electrode was short and the pulse width high, the relative neurite length was shorter. The examined samples showed an almost constant neurite length up to a charge density of 3.8 μC·cm^{-2}·phase^{-1} ($\bar{\sigma}_{samples\ 6\cdot10^{-2}-3.8\ \mu C\cdot cm^{-2}\cdot phase^{-1}}$ = 177.4 ± 1.5 μm). There were no significant differences between stimulated and unstimulated SGN culture. However, SGN stimulated at 1 mA and 400 μs pulse width formed shorter neurites (Fig. 8b) with the reduction being significant at charge densities of 3.8 – 5.4 μC·cm^{-2}·phase^{-1}.

In order to investigate the effect of ES on the morphology of the SGN, the different neuronal subtypes, i.e., monopolar, bipolar, pseudomonopolar and multipolar were quantified (Fig. 9). The distribution of the different subtypes at charge densities below 0.81 μC·cm^{-2}·phase^{-1} was comparable to the unstimulated references with no significant differences. A

Fig. 8 Relative neurite length after electrical stimulation over 24 h at different pulse widths. Current amplitude was constant at 1 mA. **a** Parameter space over different pulse widths and radii, **b** Detailed representations of three pulse widths with corresponding charge density at the respective stimulation site, mean ± standard error of the mean (SEM). $n = 1 - 59$. *$p < 0.05$

significant increase ($p < 0.01$) in monopolar SGN was observed at a charge density of 0.81 μC·cm^{-2}·phase^{-1} (Fig. 9a). At charge densities between 1.3 and 7.5 μC·cm^{-2}·phase^{-1} (at 0.44 mA (Fig. 9b) and 0.88 mA (not shown)), the percentage of pseudomonopolar SGN was significantly higher ($p < 0.05$) than that of bipolar SGN. With an increase in charge density over 2.4 μC·cm^{-2}·phase^{-1} at an amplitude of 1.0 mA and 2.0 mA, the percentage of monopolar SGN increased to approximately 100% (Fig. 9c, d). The average distribution of the four morphology groups in the unstimulated references is described below: monopolar 59.0 ± 1.8%, bipolar 17.3 ± 2.0%, pseudomonopolar 23.2 ± 1.6% and multipolar 0.48 ± 0.30%.

Discussion

In this study, we investigated the influence of in vitro electrical stimulation on dissociated SGN. For this purpose, a special stimulation chamber providing a radial electric field was designed. This approach enabled parameter screening with different charge densities at the site of individual cells within one experiment. Cells at the same distance from the central electrode should be exposed to the same strength of electrical field and therefore, to the same charge density. To facilitate evaluation, a grid providing equidistant lines around the central electrode was fixed to the bottom of the cell culture dish.
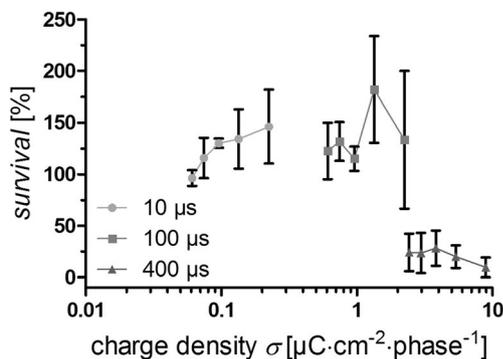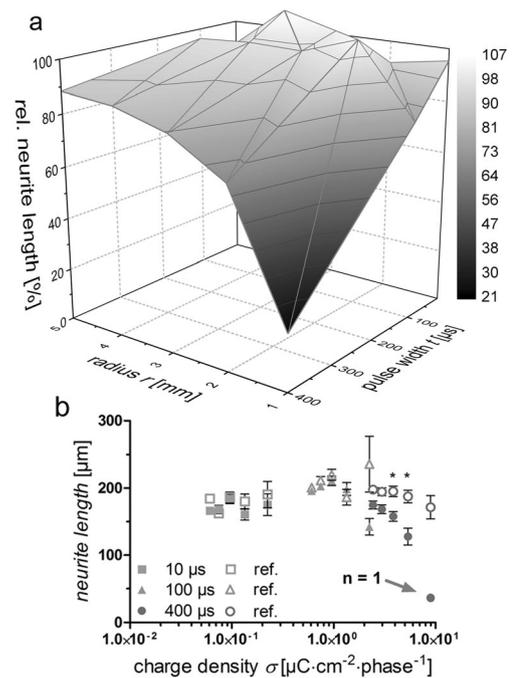

Fig. 7 Relative SGN survival at 1 mA with different pulse widths after 24 h of stimulation. The measuring points of the individual currents relate to the distance to the central electrode and can be read from right to left as follows: [1, 2, 3, 4, 5] mm. $n = 1 - 59$

Fig. 9 Appearance of SGN morphologies with different stimulation current amplitudes. The variability of morphology decreased with increasing stimulation current. The distribution of morphologies in the respective references is additionally provided in all parts of the figure. The corresponding unstimulated reference was statistically compared to the stimulated samples. The percentage of monopolar neurites was increased with charge density. Means ± standard error of the mean (SEM), $N = 3$, $*p < 0.05$; $**p < 0.01$; $***p < 0.001$
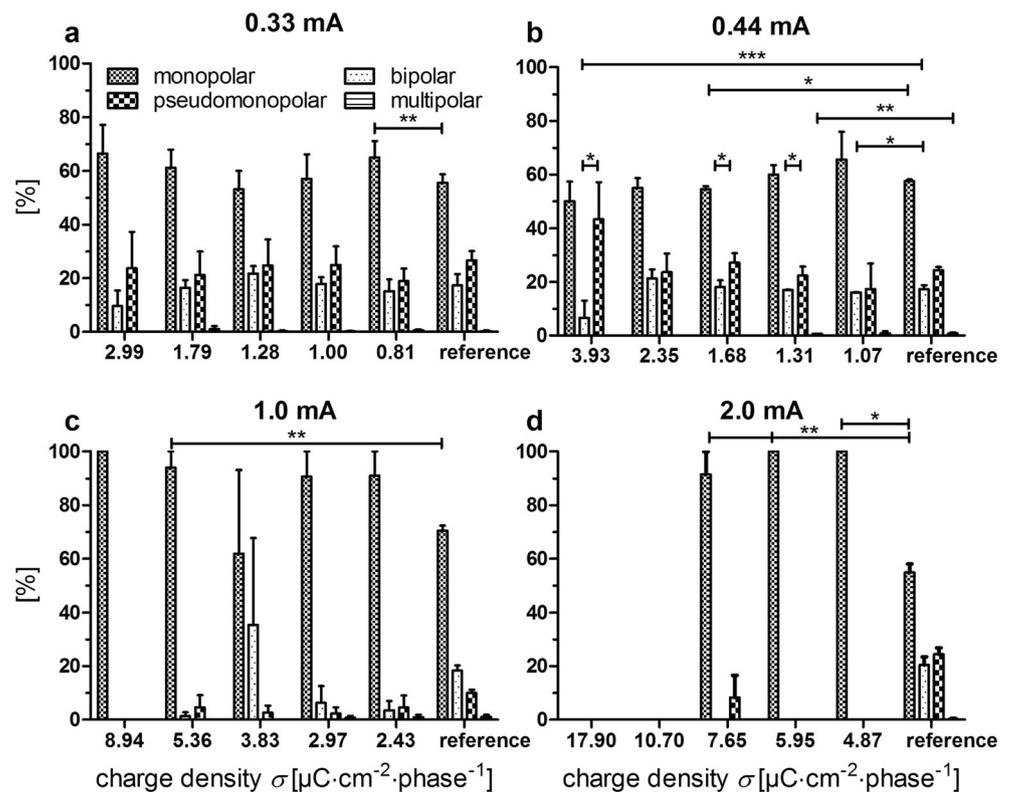
Furthermore, using biphasic rectangular pulses at constant current, it was possible to mimic stimulation of CI at least to some extent. To define stimulation parameters for the experiments, software and brochures of CI manufacturers were evaluated for parameters being in fact used during CI stimulation (for overview see Table 2).

The maximum parameters chosen were set for maximum current (2.0 mA; OTICON MEDICAL) and pulse width (400 μs; COCHLEAR), as per different CI manufacturers, knowing that the combination of both maximum values provides much higher charge densities than actually used for CI stimulation. Due to the pseudo-monophasic electrical stimulation from the manufacturer OTICON MEDICAL, a direct comparison among the manufacturers is not possible. In order to investigate possible negative effects of electrical stimulation on SGN, other factors that could damage the cells should be excluded. We were able to exclude the possible increase in temperature due to electrical stimulation as consequently associated with thermal damage of the cells, because the measured temperature changes (± 0.1 °C) were within the temperature variation of the incubator.

To ensure close to equal distribution of the cells around the centre electrode, the cell suspension was pipetted in the centre of the dishes. As the radius increases, the number of cells at equal distance increases (Fig. 3a). This increase in cell number is smaller than expected, indicating that the number of cells per area is higher close to the centre compared to more distant areas. As this is the case for stimulated samples and references, and the results were always normalised to the respective references,

this should not have influenced presented results. When comparing neurite length in experiments with the electrode (no stimulation) and without the electrode in the dishes, shorter neurites were found at 4- and 5-mm distance from the centre of present electrodes. This difference cannot be explained by the use of the hydrophobic barrier or by the electrode material. The hydrophobic barrier is still about 5 mm away and was used earlier successfully in neuronal cell culture (Shea et al. 2010). Even in the references without electrodes, the hydrophobic barrier was used and should therefore have the same influence here. As the cells in a radius of 1 mm from the centre electrode are much closer to the electrode material than the ones with reduced neurite length, the influence of the electrode can be excluded. Furthermore, the electrode material platinum/iridium is classified as biocompatible (de Haro et al. 2002; Habel 2004; Burblies et al. 2016).

Due to the design of the stimulation chamber, the applied currents lead to different charge densities at different positions and certain charge density ranges were covered by different currents. With increasing distance from the centre electrode, the charge density decreases as depicted in Fig. 1c. We expected that the same charge density leads to similar cell survival. However, this could not be verified by our results. The same charge density of about 0.75 μC·cm^{-2}·phase^{-1} led to different rel. survival rates. For example, with an amplitude of 0.25 mA and a radius of 4 mm, a rel. survival rate of 175% was determined. In contrast, with an amplitude of 0.084 mA and a radius of 1 mm, a rel. survival rate of 74% was determined.

Table 2 Cochlear implant stimulation parameters of different manufacturers. Data were collected from the following software versions or from the brochures of the manufacturers (reading 18.09.2017) [a]Soundwave Professional suite, [b]CustomSound 4.4, [c]Maestro M7, [d]COCHLEAR, Nucleus Technical Reference Manual (1999). [e]Instruction manual of MEDEL, Mi1200 Synchrony, [f]Manual of COCHLEAR, Nucleus CI512 (2016), [g]Manual of OTICON MEDICAL, Neuro Zti-Cochlear-Implant (2015). OTICON MEDICAL uses a pseudo-monophasic stimulation that works with an anodic-first pulse with a passive discharge as second phase

Manufactures	OTICON MEDICAL	MEDEL	COCHLEAR	ADVANCED BIONICS
Current [µA]	100–2000[g]	up to 1250[e]	10.2–1750[d, f]	N/A
Pulse width [µs]	8 – 250[g]	up to 203.8[e]	9.6 – 400[b, f]	18 – 229[a]
Frequency/channel [Hz]	500 – 1040[g]	193 – 4225[c]	250 – 3500[b]	91 – 3721[a]
Interpulse Delay [µs]	N/A	2.1 – 30[c]	N/A	N/A

N/A no valid information available

These amplitude and radius data all result in the charge density of $0.75~\mu C \cdot cm^{-2} \cdot phase^{-1}$. Thus, our results indicate a possible effect of the distance between the cells and electrode on SGN survival. Accordingly, the stimulation chamber is suitable as a screening tool and is used for further experiments. Based on our results, the charge density has an influence on SGN survival and neurite outgrowth.

The resulting rel. cell survival was fitted by a sigmoidal survival curve (Fig. 5). Based on this curve, limits can be estimated as follows: under $1.8~\mu C \cdot cm^{-2} \cdot phase^{-1}$ stimulation is safe and survival is comparable to that of the respective references. Above $3.8~\mu C \cdot cm^{-2} \cdot phase^{-1}$, nearly no cells survive. Apart from this, cell survival was lowest at the shortest distance from the central electrode for nearly all applied currents. Possible reasons for this could be of physical as well as chemical nature, as changes in pH or water electrolysis should be considered upon applying current to the tissue culture medium (Cogan et al. 2016). However, during the experiments, no changes in colour of the medium containing phenolsulfonephthalein and no visible gas bubble formation at the central electrode were observed. Electrolytic reactions can be excluded up to a charge density of $\sim 750~\mu C \cdot cm^{-2}$ (Brummer and Turner 1975). Other reasons for the sensitive response to higher charge densities could be the accumulation of metal ions, which have a toxic effect (Roth and Salvi 2016).

Neuronal morphology data revealed a decrease in diversity with increasing charge density (Fig. 9).The percentage of monopolar SGN increased significantly at charge densities above $2.4~\mu C \cdot cm^{-2} \cdot phase^{-1}$. Chronic noise exposure in patients can damage the cochlea to such an extent that mainly monopolar SGN (69%) can be found in this region (Liu et al. 2015). This indicates that neurons with monopolar morphology are more resistant to external influences (in our case: electrical stimulation). Spiral ganglion neurons consist mainly of type I (myelinated and connected to inner hair cells) and type II (unmyelinated and connected to outer hair cells) neurons (Nayagam et al. 2011). Based on their morphology or based on immunocytochemical detection of marker proteins, the two types can be differentiated. In the present investigations, only the morphology of the SGN was considered. A specific assignment of the bipolar SGN to types I or II can only be done by immunocytochemical labeling (Barclay et al. 2011). The cell culture was carried out with disassociated neonatal rats (P3–4). Mechanical and enzymatic stress may influence the ratio of the morphologies. The age of the animals also plays a decisive role (Chiong et al. 1993). In the neonatal spiral ganglion, more type II neurons can be found than in the adult (Chiong et al. 1993). Up to a charge density of $1.3~\mu C \cdot cm^{-2} \cdot phase^{-1}$, the percentage of bipolar neurons was lower than pseudomonopolar neurons. Other studies have confirmed such sensitivity by showing that moderate inner hair cell loss and type I (being mainly bipolar) SGN degeneration have been shown to have little impact on hearing in noise when the outer hair cells are still intact (Dabdoub et al. 2016; Lobarinas et al. 2016). The loss of diversity over $2.4~\mu C \cdot cm^{-2} \cdot phase^{-1}$ also indicates that bipolar and pseudomonopolar neurons are more sensitive than the monopolar SGN (Kiang et al. 1982; Liu et al. 2015). The neuronal morphology differed slightly from the percentages known in the literature (Whitlon et al. 2007; Schwieger et al. 2015). This is due to the fact that the SGN without neurites were not counted and thus a smaller total amount was determined. Nevertheless, monopolar SGNs were also the most counted. Whether electrical stimulation can alter the ratio of type I to type II SGN is currently unclear as only the morphologies of the neurons have been considered. Therefore, this should be investigated in further studies.

When applying 1 mA, the neurite length increased linearly ($\alpha = 0.05$) with increasing distance from the centre electrode and thus a decrease in charge density (Fig. 6b). It is remarkable that even though only about 24% of cells survived (1 mA, 5 mm from centre), neurite length appeared still relatively unaffected. The variation of shorter pulse widths (10 – 100 µs) induced no significant difference in survival and neurite outgrowth of SGN, but there is a slight positive trend (increased survival and longer neurites) in the shorter pulse widths. According to the published results, electrical stimulation can influence the neurite length (Shen et al. 2016). Shen's group also demonstrated in an in vitro experiment that biphasic electrical stimulation after 24 h and 50 µA may negatively

impact neurite outgrowth. On the other hand, it has been shown that exogenous electrical stimulation may have protective effects on spinal cord neurons (Liu et al. 2018). Thus, electrical stimulation can be either protective or toxic. Other factors such as the distance to the electrode must be observed if the effect is positive or negative. Parameters for safe stimulation of cortical neurons using platinum electrodes in vivo have been determined earlier (Shannon 1992). The illustration (Fig. 10) separates the range of electrical stimulation into a safe and an unsafe area by the factor k. At a value of $k = 2$, the line shifts to an area where electrical stimulation damage is expected. According to Shannon, no damage was observed at $k = 1.5$. Based on Shannon's results, the parameters for safe stimulation were mathematically refined by considering chemical and physical levels (Hudak et al. 2017). Due to the passivation of the platinum, the proteins present and chloride ions, the k value was increased to 1.75 (Hudak et al. 2017). To compare our parameters and results with the published limits, pulses of our study were plotted into Shannon's model of charge Q and charge density σ (Fig. 10).

Using this approach, it should be possible to estimate which pulses can be considered safe or unsafe (Merrill et al. 2005). Charge distribution within the culture dish is limited by the filling level of the medium. Having a cylindrical central electrode with 1-mm free surface length and a fluid level of initially 2 mm (reduced by about 6% during culture), it was assumed that the electric field spreads cylindrically from the central electrode
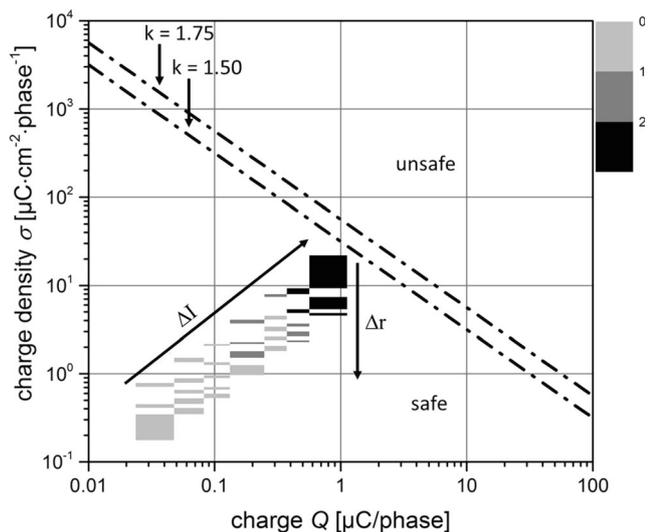

Fig. 10 Charge Q vs. charge density σ according to Merrill et al. (2005). The dashed lines indicate the safety limits for electrical stimulation according to the two models (model of Shannon (1992) $k = 1.50$ and model of Hudak et al. (2017) $k = 1.75$). Below the dotted lines is the safe and above unsafe stimulation range described in the models. The additional data points shown here correspond to the stimulating parameters used in this study. Legend: 0 (light grey) = safe stimulation < 1.8 $\mu C \cdot cm^{-2} \cdot phase^{-1}$; 1 (dark grey) = 1.8 – 3.8 $\mu C \cdot cm^{-2} \cdot phase^{-1}$; 2 (black) = unsafe stimulation > 3.8 $\mu C \cdot cm^{-2} \cdot phase^{-1}$. Δr = Variation of the radius from central electrode, ΔI = Variation of the current. In this diagram, the applied pulses are plotted at a pulse width of 400 μs

to simplify the model in the current approach. The pulses used in the current study should theoretically be in the safe area according to Hudak's calculations. The central electrode with an area of 1.56 ± 0.43 mm^2 and a maximum pulse width of 400 μs could, according to the model, be operated at a safe amplitude of 2.3 mA. However, the current investigations revealed strong influence on cell survival as well as neurite outgrowth that was seen even at an amplitude of 1 mA and otherwise the same pulse width. To explain these differences, it should be noted that the results of Shannon were based on animal testing, Hudak's limits on mathematical corrections of Shannon's limits and the results in the current study were obtained in in vitro experiments. As the native environment is protective for cells (Coco et al. 2007), higher safety limits are to be expected in vivo. Therefore, it is necessary to define separate limits for both in vivo and in vitro. After reviewing the current data, the k value would have to be reduced to 0.420 for in vitro stimulation. Accordingly, dissociated cells in mixed culture might have less endogenous protection against such conditions. On the other side, in vitro conditions are better controlled, and currents' limits may be exceeded in vivo due to unpredictable biological factors. In general, it should be noted that there are also other factors that can influence the safety stimulating limit, such as duty cycle, repetition rate and current density (Cogan et al. 2016).

In summary, the developed stimulation chamber and setup can be used to screen parameters of electrical stimulation in vitro. The presented results provide parameter sets/charge densities that can be used to study in vitro the effect of damage to SGN by electrical stimulation and to screen for protection strategies to maintain and protect residual hearing in patients with implants. Furthermore it has to be noted that the setup can also be used to investigate the effect of electrical stimulation to hair cells and other cell types.

Compliance with Ethical Standards

Conflict of Interest The authors declare that they have no conflict of interest.

References

Barclay M, Ryan AF, Housley GD (2011) Type I vs type II spiral ganglion neurons exhibit differential survival and neuritogenesis during cochlear development. Neural Dev 6:33. https://doi.org/10.1186/1749-8104-6-33

Brummer SB, Turner MJ (1975) Electrical stimulation of the nervous system: the principle of safe charge injection with noble metal

electrodes. Bioelectrochem Bioenerg 2:13–25. https://doi.org/10.1016/0302-4598(75)80002-X

Budni J, Molz S, Dal-Cim T, Martín-de-Saavedra M, Dolores E et al (2018) Folic acid protects against glutamate-induced excitotoxicity in hippocampal slices through a mechanism that implicates inhibition of GSK-3β and iNOS. Mol Neurobiol 55:1580–1589. https://doi.org/10.1007/s12035-017-0425-6

Burblies N, Schulze J, Schwarz H-C, Kranz K, Motz D, Vogt C, Lenarz T, Warnecke A, Behrens P (2016) Coatings of different carbon nanotubes on platinum electrodes for neuronal devices: preparation, cytocompatibility and interaction with spiral ganglion cells. PLoS One 11:e0158571. https://doi.org/10.1371/journal.pone.0158571

Chiong CM, Burgess BJ, Nadol JB (1993) Postnatal maturation of human spiral ganglion cells: light and electron microscopic observations. Hear Res 67:211–219. https://doi.org/10.1016/0378-5955(93)90249-Z

Coco A, Epp SB, Fallon JB, Xu J, Millard RE, Shepherd RK (2007) Does cochlear implantation and electrical stimulation affect residual hair cells and spiral ganglion neurons? Hear Res 225:60–70. https://doi.org/10.1016/j.heares.2006.12.004

Cogan SF, Ludwig KA, Welle CG, Takmakov P (2016) Tissue damage thresholds during therapeutic electrical stimulation. J Neural Eng 13:021001. https://doi.org/10.1088/1741-2560/13/2/021001

Dabdoub A, Fritzsch B, Popper AN, Fay RR (2016) The primary auditory neurons of the mammalian cochlea, 52nd edn. Springer, Berlin Heidelberg, p 234

de Haro C, Mas R, Abadal G, Muñoz J, Perez-Murano F, Domínguez C (2002) Electrochemical platinum coatings for improving performance of implantable microelectrode arrays. Biomaterials 23:4515–4521. https://doi.org/10.1016/S0142-9612(02)00195-3

Dziewas R, Stellato R, van der Tweel I, Walther E, Werner CJ, et al (2018) Pharyngeal electrical stimulation for early decannulation in tracheotomised patients with neurogenic dysphagia after stroke (PHAST-TRAC): a prospective, single-blinded, randomised trial. Lancet Neurol doi: https://doi.org/10.1016/S1474-4422(18)30255-2, 17, 849, 859

Gillespie LN, Clark GM, Bartlett PF, Marzella PL (2001) LIF is more potent than BDNF in promoting neurite outgrowth of mammalian auditory neurons in vitro. Neuroreport 12:275–279. https://doi.org/10.1097/00001756-200102120-00019

Habel B (2004) Elektrische Stimulation von Zellen und Geweben am besonderen Beispiel von Knochenzellen. Dissertaion, Humboldt-Universität zu Berlin

Hartshorn DO, Miller JM, Altschuler RA (1991) Protective effect of electrical stimulation in the deafened Guinea pig cochlea. Otolaryngol Neck Surg 104:311–319. https://doi.org/10.1177/019459989110400305

Helbig S, Adel Y, Rader T, Stöver T, Baumann U (2016) Long-term hearing preservation outcomes after Cochlear implantation for electric-acoustic stimulation. Otol Neurotol 37:e353–e359. https://doi.org/10.1097/MAO.0000000000001066

Hudak EM, Kumsa DW, Martin HB, Mortimer JT (2017) Electron transfer processes occurring on platinum neural stimulating electrodes: calculated charge-storage capacities are inaccessible during applied stimulation. J Neural Eng 14:046012. https://doi.org/10.1088/1741-2552/aa6945

Jurawitz M-C, Büchner A, Harpel T, Schüssler M, Majdani O, Lesinski-Schiedat A, Lenarz T (2014) Hearing preservation outcomes with different Cochlear implant electrodes: nucleus® HybridTM-L24 and nucleus FreedomTM CI422. Audiol Neurotol 19:293–309. https://doi.org/10.1159/000360601

Kiang N, Rho J, Northrop C, Liberman M, Ryugo D (1982) Hair-cell innervation by spiral ganglion cells in adult cats. Science 217:175–177. https://doi.org/10.1126/science.7089553

Kopelovich JC, Reiss LAJ, Etler CP, Xu L, Bertroche JT, Gantz BJ, Hansen MR (2015) Hearing loss after activation of hearing

preservation Cochlear implants might be related to afferent Cochlear innervation injury. Otol Neurotol 36:1035–1044. https://doi.org/10.1097/MAO.0000000000000754

Kujawa SG (2006) Acceleration of age-related hearing loss by early noise exposure: evidence of a misspent youth. J Neurosci 26:2115–2123. https://doi.org/10.1523/JNEUROSCI.4985-05.2006

Kujawa SG, Liberman MC (2009) Adding insult to injury: cochlear nerve degeneration after "temporary" noise-induced hearing loss. J Neurosci 29:14077–14085. https://doi.org/10.1523/JNEUROSCI.2845-09.2009

Leake PA, Hradek GT, Rebscher SJ, Snyder RL (1991) Chronic intracochlear electrical stimulation induces selective survival of spiral ganglion neurons in neonatally deafened cats. Hear Res 54:251–271. https://doi.org/10.1016/0378-5955(91)90120-X

Liberatore F, Bucci D, Mascio G, Madonna M, Di Pietro P et al (2017) Permissive role for mGlu1 metabotropic glutamate receptors in excitotoxic retinal degeneration. Neuroscience 363:142–149. https://doi.org/10.1016/j.neuroscience.2017.09.005

Liu W, Edin F, Atturo F, Rieger G, Löwenheim H, Senn P, Blumer M, Schrott-Fischer A, Rask-Andersen H, Glueckert R (2015) The pre- and post-somatic segments of the human type I spiral ganglion neurons - structural and functional considerations related to cochlear implantation. Neuroscience 284:470–482. https://doi.org/10.1016/j.neuroscience.2014.09.059

Liu M, Yin C, Jia Z, Li K, Zhang Z, Zhao Y, Gong X, Liu X, Li P, Fan Y (2018) Protective effect of moderate exogenous electric field stimulation on activating Netrin-1/DCC expression against mechanical stretch-induced injury in spinal cord neurons. Neurotox Res 34:285–294. https://doi.org/10.1007/s12640-018-9885-3

Lobarinas E, Salvi R, Ding D (2016) Selective inner hair cell dysfunction in chinchillas impairs hearing-in-noise in the absence of outer hair cell loss. JARO JARO - J Assoc Res Otolaryngol 17:89–101. https://doi.org/10.1007/s10162-015-0550-8

Long Y, Wei H, Li J, Yao G, Yu B, et al (2018) Effective Wound Healing Enabled by Discrete Alternative Electric Fields from Wearable Nanogenerators. ACS Nano acsnano.8b07038. doi: https://doi.org/10.1021/acsnano.8b07038

Lousteau RJ (1987) Increased spiral ganglion cell survival in electrically stimulated, deafned guinea pig cochleae. Laryngoscope 97:836–842. https://doi.org/10.1288/00005537-198707000-00012

Merrill DR, Bikson M, Jefferys JGR (2005) Electrical stimulation of excitable tissue: design of efficacious and safe protocols. J Neurosci Methods 141:171–198. https://doi.org/10.1016/j.jneumeth.2004.10.020

Mitchell A, Miller JM, Finger PA, Heller JW, Raphael Y, Altschuler RA (1997) Effects of chronic high-rate electrical stimulation on the cochlea and eighth nerve in the deafened guinea pig. Hear Res 105:30–43. https://doi.org/10.1016/S0378-5955(96)00202-X

Nayagam B, Muniak M, Ryugo D (2011) The spiral ganglion: connecting the peripheral and central auditory systems. Hear Res 278:2–10. https://doi.org/10.1016/j.heares.2011.04.003

Olney JW, Ho O, Rhee V (1971) Cytotoxic effects of acidic and sulphur containing amino acids on the infant mouse central nervous system. Exp Brain Res 14:61–76. https://doi.org/10.1007/BF00234911

Puel J-L, Ruel J, D Aldin CG, Pujol R (1998) Excitotoxicity and repair of cochlear synapses after noise-trauma induced hearing loss. Neuroreport 9:2109–2114. https://doi.org/10.1097/00001756-199806220-00037

Reich U, Warnecke A, Szczepek AJ, Mazurek B, Olze H (2015) Establishment of an experimental system to study the influence of electrical field on cochlear structures. Neurosci Lett 599:38–42. https://doi.org/10.1016/j.neulet.2015.05.027

Rosso IM, Crowley DJ, Silveri MM, Rauch SL, Jensen JE (2017) Hippocampus glutamate and N-acetyl aspartate markers of excitotoxic neuronal compromise in posttraumatic stress disorder.

Neuropsychopharmacology 42:1698–1705. https://doi.org/10.1038/npp.2017.32

Roth JA, Salvi R (2016) Ototoxicity of divalent metals. Neurotox Res 30:268–282

Roxo RS, Xavier VB, Miorin LA, Magalhães AO, dos Santos Sens YA et al (2016) Impact of neuromuscular electrical stimulation on functional capacity of patients with chronic kidney disease on hemodialysis. J Bras Nefrol. https://doi.org/10.5935/0101-2800.20160052

Santa Maria PL, Domville-Lewis C, Sucher CM, Chester-Browne R, Atlas MD (2013) Hearing preservation surgery for Cochlear implantation—hearing and quality of life after 2 years. Otol Neurotol 34:526–531. https://doi.org/10.1097/MAO.0b013e318281e0c9

Scheper V, Paasche G, Miller J, Warnecke A, Berkingali N et al (2009) Effects of delayed treatment with combined GDNF and continuous electrical stimulation on spiral ganglion cell survival in deafened guinea pigs. J Neurosci Res 87:1389–1399. https://doi.org/10.1002/jnr.21964

Schwieger J, Warnecke A, Lenarz T, Esser K-H, Scheper V (2015) Neuronal survival, morphology and outgrowth of spiral ganglion neurons using a defined growth factor combination. PLoS One 10:e0133680. https://doi.org/10.1371/journal.pone.0133680

Schwieger J, Esser K-H, Lenarz T, Scheper V (2016) Establishment of a long-term spiral ganglion neuron culture with reduced glial cell number: effects of AraC on cell composition and neurons. J Neurosci Methods 268:106–116. https://doi.org/10.1016/j.jneumeth.2016.05.001

Shannon RV (1992) A model of safe levels for electrical stimulation. IEEE Trans Biomed Eng 39:424–426. https://doi.org/10.1109/10.126616

Shea GKH, Tsui AYP, Chan YS, Shum DKY (2010) Bone marrow-derived Schwann cells achieve fate commitment – a prerequisite for remyelination therapy. Exp Neurol 224:448–458. https://doi.org/10.1016/j.expneurol.2010.05.005

Shen N, Liang Q, Liu Y, Lai B, Li W, Wang Z, Li S (2016) Charge-balanced biphasic electrical stimulation inhibits neurite extension of spiral ganglion neurons. Neurosci Lett 624:92–99. https://doi.org/10.1016/j.neulet.2016.04.069

Skarzynski H, van de Heyning P, Agrawal S, Arauz SL, Atlas M, Baumgartner W, Caversaccio M, de Bodt M, Gavilan J, Godey B, Green K, Gstoettner W, Hagen R, Han DM, Kameswaran M, Karltorp E, Kompis M, Kuzovkov V, Lassaletta L, Levevre F, Li Y, Manikoth M, Martin J, Mlynski R, Mueller J, O'Driscoll M, Parnes L, Prentiss S, Pulibalathingal S, Raine CH, Rajan G, Rajeswaran R, Rivas JA, Rivas A, Skarzynski PH, Sprinzl G, Staecker H, Stephan K, Usami S, Yanov Y, Zernotti ME, Zimmermann K, Lorens A, Mertens G (2013) Towards a consensus on a hearing preservation classification system. Acta Otolaryngol 133:3–13. https://doi.org/10.3109/00016489.2013.869059

Stalmann U (2015) Altersabhängige Degeneration und Lärmempfindlichkeit des Corti-Organs bei tauben Otof-Knockout-Mäusen. Dissertation, Georg-August-Universität zu Göttingen

Sucher NJ, Lipton SA, Dreyer EB (1997) Molecular basis of glutamate toxicity in retinal ganglion cells. Vis Res 37:3483–3493. https://doi.org/10.1016/S0042-6989(97)00047-3

Warnecke A, Sasse S, Wenzel GI, Hoffmann A, Gross G, Paasche G, Scheper V, Reich U, Esser KH, Lenarz T, Stöver T, Wissel K (2012) Stable release of BDNF from the fibroblast cell line NIH3T3 grown on silicone elastomers enhances survival of spiral ganglion cells in vitro and in vivo. Hear Res 289:86–97. https://doi.org/10.1016/j.heares.2012.04.007

Whitlon D, Grover M, Tristano J, Williams T, Coulson MT (2007) Culture conditions determine the prevalence of bipolar and monopolar neurons in cultures of dissociated spiral ganglion. Neurosci 146:833–840. https://doi.org/10.1016/j.neuroscience.2007.01.036